AADE-14-FTCE-40

Is the Wellbore Prepared "Enough" for Cementing?—Finding Answers using Electrochemical Impedance Spectroscopy

Venkata Gopala Rao Palla, PKS Sairam, and Abhimanyu Deshpande, Halliburton

Abstract

Preparing the casing surface and the wellbore to receive cement slurry is crucial during cementing operations. If oil-based mud (OBM) is used during drilling, the casing surface can be rendered oil-wet. A clean casing surface before cementing is important for providing proper shear bond strength (SBS) and long-term wellbore integrity. Spacer fluids are typically pumped before cement placement to clean the casing and wellbore surfaces and to help avoid direct contact between cement and muds. A reliable experimental technique that can quantify wetting characteristics of the casing surface and estimate the contact time necessary to clean the oil film can be helpful when designing an effective cement job.

This paper describes experiments using electrochemical impedance spectroscopy (EIS) for surface wettability measurements. EIS measures the impedance of the system over a range of frequencies. This impedance spectrum is modeled to fit an equivalent electric circuit, which mimics the actual physics to quantify the different processes of the system. Experimentally, the pump rate is simulated using an equivalent wall shear by tuning the rev/min of a concentric Couette flow. It is observed that the cleaning time under similar shear application using the designed spacer varied 4 to 5 fold for different aromatic-based OBMs with the same oil-water ratio and densities ranging from 10 to 16 lb/gal. This work demonstrates how the spacer volume, pump rate, and other operating parameters can be accurately engineered for the job. The advantage of being able to measure at high-pressure/high-temperature (HP/HT) conditions non-invasively makes this technique useful for real-time measurements and helps improve the quality of downhole assurance.

Introduction

Preparing the casing surface and the wellbore, for receiving the cement slurry, forms one of the crucial steps for successful zonal isolation. The wellbore is circulated with drilling mud at least two wellbore volumes before pumping any other cementing fluids to facilitate good conditioning of the drilling mud, thereby facilitating the easy removal of mud. The drilling muds can be water-based or oil-based. Water-based-mud (WBM) is usually a homogeneous blend of water, clay, and other chemicals. An OBM contains droplets of fresh water or salt solution dispersed in an oil-based continuous phase. The stability of these emulsions depends on various factors, such as oil-water ratio, pH, temperature, surfactant loading, and other various factors. Rossen and Kohn (1984), Quintero et al. (1976), and Robbins (1976) provide a detailed understanding on micro-emulsions and their phase behavior under different conditions.[1-3]

For drilling the majority of deeper wellbores, OBMs are used for their inherent advantages. OBMs are used for achieving faster drilling rates, with lower drill-pipe torque and drag, less bit balling, as well as reduced differential sticking. Although OBMs are expensive, their use is justified particularly while drilling through troublesome shale formations, which have the tendency to swell if drilled using WBMs; deep, high-temperature formations, which might dehydrate the WBMs; water soluble zones; and producing zones.[4-5] The density of mud can range anywhere between 7 and 22 lb/gal. Although the density of the OBM is sensitive to temperatures, it does not dehydrate like WBM.

When OBM is used as a drilling fluid, the formation surface and the casing surface are rendered oil-wet. Depending on formation permeability, a small layer of mud cake deposits on the formation surface. Also, there is a chance of incompatibility if cement directly contacts OBM.

The spacer fluids[6-10] are pumped before introducing the cement slurry. While designing the density and rheological parameters of the spacer, various parameters, such as residual shear stress (RSS) of the mud cake, pump rate, density, rheology of mud, and wellbore geometry are considered. The spacer thus prepared with the desired density and rheological parameters is optimized for surfactant concentration by taking a predetermined mixture of OBM and spacer and continuously adding surfactant while mixing in a jar until a predetermined value of conductivity is achieved.

A spacer fluid serves two purposes. Firstly, it acts as a barrier between cement slurry and OBM and displaces the mud. Secondly, it erodes the mud cake and cleans the casing surface. A robust three-dimensional (3D) displacement simulator can provide an estimate of how much spacer volume must be pumped to displace the mud and avoid direct contact between the OBM and cement. However, whether the pumped volume of spacer, at the desired pump rate, is sufficient to clean the casing and formation surface cannot be answered using displacement simulations.

For a proper bonding[11-13] between the casing surface and cement, the casing surface must be water-wet before receiving the cement. Hence, a laboratory technique, which can quantify the wetting characteristic of the surface under given operating conditions, such as temperature, pressure, and shear rates, using the designed spacer for a given OBM, is helpful for designing the cementing job much more efficiently.

In the following sections, a non-invasive technique using EIS to measure surface wettability is described with theoretical background and preliminary results obtained from the laboratory. Design details of the apparatus, which is built based on the previous concept, are also briefly discussed.

Double-Layer Capacitance

When a charged electrode contacts an electrolyte, oppositely charged ions adsorb on the electrode surface. Next to this layer of ions, similarly charged ions adsorb because of the columbic forces. Ions from the bulk liquid are loosely distributed as the distance from the electrode surface increases. The layers of ions sticking to the electrode surface are known as a double layer,[14] and the charged electrode is separated from the ions in the bulk liquid by a few angstroms. Because charges separated by an insulator form a capacitor, a charged electrode immersed in an electrolyte acts like a capacitor. **Fig. 1** illustrates the schematic arrangement of ions surrounding the interface between the electrode and electrolyte.

It is estimated that this capacitance will be approximately 20 to 60 μF per 1 cm^2 of electrode area. However, the value of the double-layer capacitance depends on many variables, such as electrode potential, temperature, ionic concentrations, types of ions, oxide layers, electrode roughness, impurity adsorption, etc.

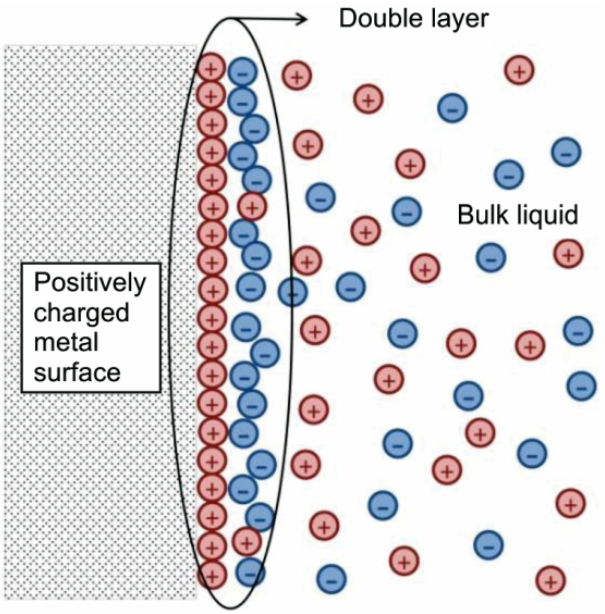

Fig. 1—Schematic of ions distributed around a charged surface.

Characterizing the Surface

It is well-known that the capacitance depends on the dielectric constant of the medium involved. Water has a dielectric constant of 80, while oils have dielectrics within the range of 2 to 3. Hence, it is expected that the double-layer capacitance, if measured properly, can vary by almost 40 fold when the wetting fluid of the surface is changed from water-based to oil-based. The technique this paper describes is based on this principle. The measurement technique is known as EIS.

EIS

EIS is the study of response of a physical system to the application of the periodic alternating current (AC) signal of small amplitude over a range of frequencies.[15] EIS is used for characterizing electrochemical systems and is widely used for evaluating coatings.[16-18] For an applied sinusoidal input E_t as in Eq. 1, the resultant current I_t is of the form shown in Eq. 2. The current and applied voltage signals differ by a phase angle depending on the type of physical processes or elements involved within the system under study. The magnitude ratio of applied voltage and resultant current provides the magnitude of the impedance, Z_0 in Eq. 3. The phase angle, φ, provides the real and imaginary component of the impedance. Both the magnitude and phase angle of the impedance are functions of frequency.

$$E_t = E_0 \, sin(\omega t) \tag{1}$$

$$I_t = I_0 \, sin\,(\omega t + \varphi) \tag{2}$$

$$Z(\omega) = Z_0 \left(cos(\varphi) + i \, sin(\varphi)\right) \tag{3}$$

The analysis of the physical system response, using EIS, provides information about the interface, its structure, and reactions occurring there.[19] **Table 1** shows the transient response and frequency dependent impedance of different electrical components to an applied sinusoidal signal. For the resistor, the impedance is not a function of applied frequency. The impedance of the capacitor is inversely proportional to the frequency. The impedance of an inductor is directly proportional to the frequency.

Table 1—Sinusoidal Response of Electrical Components

Electrical Component	Transient Response	Impedance
Resistor, R	$E = IR$	$Z = R$
Capacitor, C	$E = \left(\frac{1}{C}\right)\int Idt$	$Z = \frac{1}{i\omega C}$
Inductor, L	$E = L\,\frac{dI}{dt}$	$Z = j\omega L$

The frequency response data obtained using EIS is represented as a Nyquist plot or Bode plot.

Bode Plot

The plots showing the magnitude and phase angle of impedance as a function of frequency, on a logarithmic scale, are known as Bode plots. A sample set of Bode plots, for various simple circuits listed in **Table 2**, are illustrated in **Fig. 2.**

Table 2—Sample Circuits with Simple Electrical Components

Circuit	Resistance Ohms	Capacitance Farads	Inductance Henry
R	1000	—	—
C	—	5×10^{-3}	—
L	—	—	25
RC Series	100	5×10^{-2}	—
RL Series	5000	—	125
LC Series	—	1×10^{-3}	625

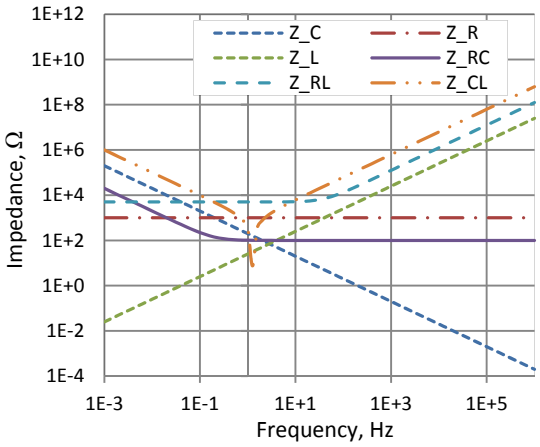

Fig. 2—Bode plots for simple circuits listed in Table 2.

Nyquist Plot

Although Bode plots provide information about the magnitude and phase angle of the impedance, it does not provide direct information about the real and imaginary components of the impedance. A plot of real vs. imaginary components of the impedance on a log-log scale is known as a Nyquist plot.

EIS Modeling

A well-connected physical system, which forms an electrically closed loop, can be represented as an equivalent electrical circuit containing different elements. The EIS data obtained for a given system is modeled into an equivalent electric circuit, and each element of the circuit represents a physical process of the system. Different processes and phenomena occurring in the system can be treated as different electrical elements, such as resistance, capacitance, Warburg impedance, inductance, etc. The overall equivalent circuit, representing the physical system as a whole, depends on how these individual elements are combined together, as well as their respective magnitudes. **Fig. 3** illustrates the sample equivalent electric circuit for a failed-paint model. **Figs. 4 and 5** illustrate the Bode and Nyquist plots for this electrical circuit, respectively.

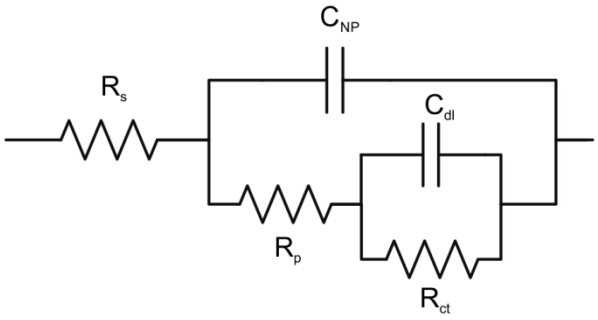

Fig. 3—Equivalent circuit for failed paint model.

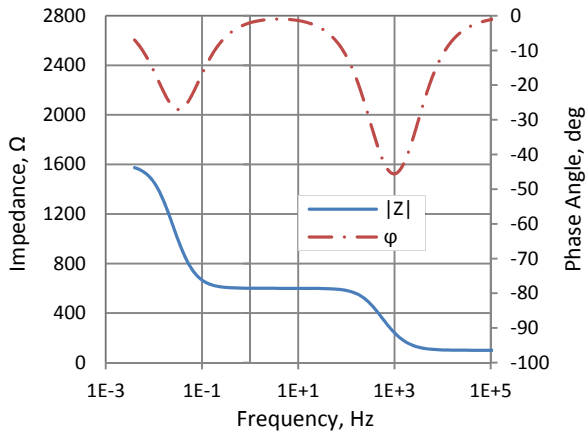

Fig. 4—Bode plots for failed paint model.

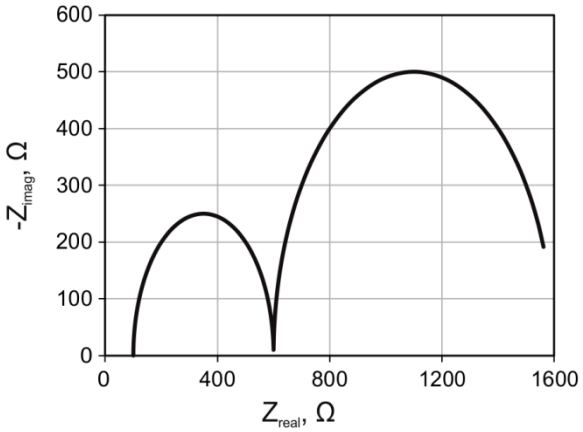

Fig. 5—Nyquist plot for failed paint model.

Proof of Concept

A small test setup is devised to prove the previous concept of quantifying wetting characteristic of the metal surface using EIS. **Fig. 6** illustrates the schematic. Two identical flat electrodes are coated with a non-aqueous film (NAF) to a predetermined fraction of the total surface. These are then immersed in a sample spacer fluid, which acts as electrolyte.

Electrodes are then connected to a commercially available Potentiostat for logging impedance spectra in the frequency range of 10 mHz to 100 kHz. This is repeated for an incremental percentage coverage of NAF from 0 to 75%, and plotted in **Fig. 7**. The obtained impedance spectra is modeled as a failed paint model as shown in Fig. 3, and as **Fig. 8** illustrates, the value of double-layer capacitance is plotted as a function of fractional NAF coverage on the electrode. The relation is determined to be close to linear, and this proves that EIS can be used to determine the fractional oil-wet or water-wet surface if properly calibrated.

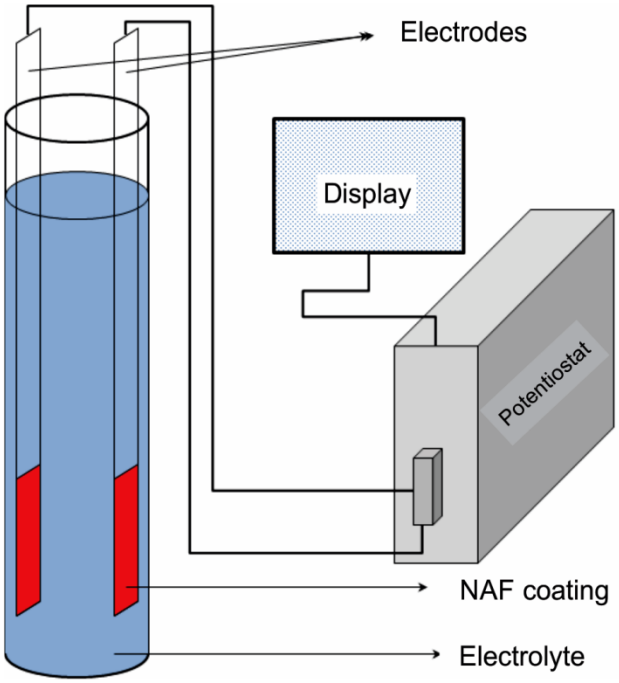

Fig. 6—Test setup for proof of concept experiments.

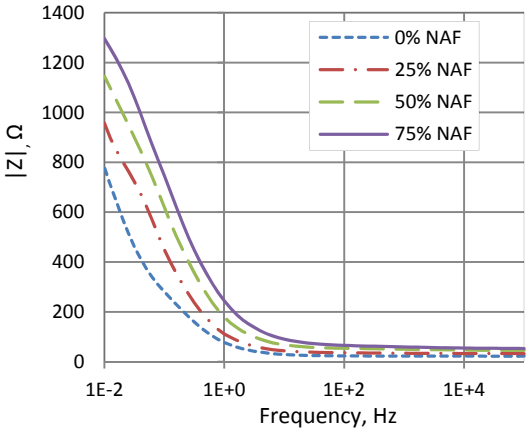

Fig. 7—Impedance spectra from test setup with varied extent of NAF coverage.

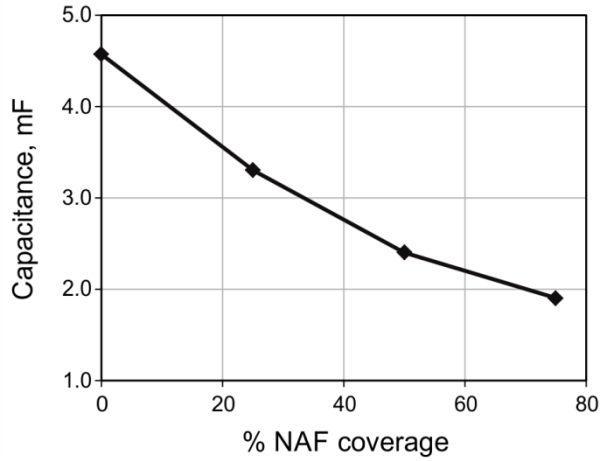

Fig. 8—Double-layer capacitance as a function of % NAF coverage.

Laboratory Test Setup

Fig. 9 illustrates the in-house developed schematic of the laboratory test apparatus. The test setup contains a cylindrical geometry for the application of shear rate at the electrode surface. Two identical curved electrodes are embedded diametrically opposite to one another on a cylindrical bob, which forms the inside diameter of the concentric annular geometry. The bob is mounted in an electric motor, which is connected to a speed-controller for rotating the bob at the desired rev/min. The open ends of the electrodes are connected to a commercially available potentiostat for EIS data logging. Although the results obtained at high temperature are not reported in this paper, the apparatus is equipped with a heater jacket to be able to perform the tests at elevated temperatures and ambient pressure.

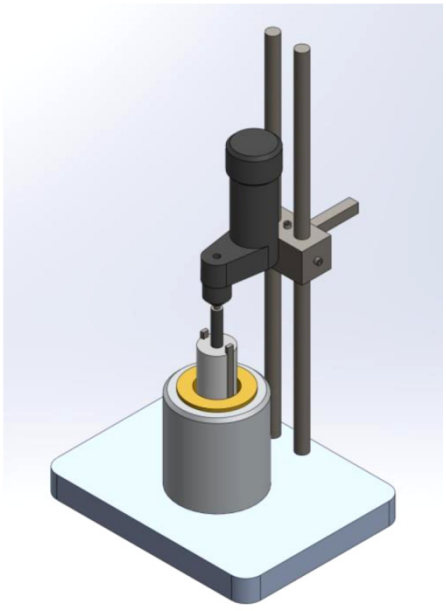

Fig. 9—Laboratory test setup for performing surface wettability studies.

Determining the Contact Time for Casing Cleaning

The objective of this work is to determine a test protocol, which can quantify the volume of spacer necessary to successfully displace the OBM and clean the oil film from the casing surface by considering the wellbore geometry, pump rates, and rheology of fluids being pumped. From literature, it is evident that the wider the annular space, and the higher the rotational speed, the higher the chances of encountering Taylor-Couette instabilities.[20] The annular geometry of the test setup is carefully optimized to avoid any flow instabilities because of high shear rates.

While performing the test, care should be taken to help ensure that there are no air bubbles entrapped at the electrode-electrolyte interface, which can cause erroneous results.

After careful experimentation using the laboratory scale apparatus, the following protocol is proposed for determining the contact time that must be maintained between the pure spacer fluid and casing, at a given pump rate, for the complete removal of OBM film from the casing surface.

1. Preparation of the spacer fluid*:* From the density and rheological properties of the OBM and flow rates to be used, the density and rheological properties of the spacer fluid are determined. A mixture of OBM and the spacer fluid from predetermined volume ratios is mixed in a jar. A combination of water-based surfactant, oil-based surfactant, and emulsifier is slowly added to the mixture, while the mixture is continuously stirred until a predetermined conductivity is achieved. The conductivity of the mixture should not change when the stirring is stopped. Once this is achieved, the spacer fluid is optimized for surfactant concentration.
2. EIS with spacer fluid for reference spectra: The cylindrical bob with electrodes is placed inside the sleeve, and the annular space is filled with the spacer fluid prepared in Step 1. The bob is rotated for approximately 30 sec to avoid any air bubbles sticking to the electrode surface, which might cause bad values in the results. Using the commercially available potentiostat, EIS is logged. This forms the reference spectra.
3. Coating the electrode surface with OBM*:* After the baseline EIS spectra with spacer fluid is taken, the bob is removed, cleaned thoroughly, and wiped dry. The bob is then dipped into a beaker filled with OBM until the electrodes are fully immersed in the mud, except for a small portion at the top, which is allotted for electrical connections. Similar to the spacer fluid, the bob is rotated for approximately 30 sec to provide a continuous OBM coating.
4. EIS before applying shear*:* The bob, which is now coated with OBM film, is dipped into the spacer solution to the desired mark. A first-cut EIS spectrum is obtained without applying any shear. The results illustrated in Figs. 10 and 11, which are described in later sections, show that the impedance values in these spectra are a few orders of magnitude higher than those in the reference spectra.
5. Application of shear and EIS data logging*:* The bob is rotated at a predetermined rev/min for a predetermined period of time. The rev/min is determined in such a way that the wall shear rate at the electrode surface obtained during this laboratory test setup is equal to the wall shear rate at the casing surface under given wellbore conditions. After the application of shear, the EIS data is logged again. The impedance spectra are then plotted on the same graph to determine how far the impedance values have reduced. The procedure of shear application and EIS data logging is repeated until the final spectra match with the reference spectra. Once the final spectra match with the reference spectra occurs, the cumulative time for which the shear is applied is counted as the contact time that must be maintained between the casing and spacer fluids to completely clean the casing surface.
6. Spacer volume calculations: The contact time obtained, as previously explained, multiplied by the pump rate, provides the volume of spacer necessary to maintain the contact time with the casing surface. However, before having an uncontaminated portion of the spacer fluid contact the casing surface, a few barrels of spacer volume is lost in the intermixing zone and channeling through OBM. The channel volume, for a given combination of pump schedule and wellbore geometry, is obtained from a robust 3D displacement simulator. Hence, the total spacer volume necessary is calculated as a sum of the volume necessary for maintaining contact time and the volume sacrificed during channeling.

Results

A large number of experiments have been performed to test different OBMs with the surface wettability measuring apparatus previously explained. Each test is repeated twice to check the repeatability, and the results are determined to be consistent. From the large pool of data obtained from different muds, the results for a few muds, where the required contact time is markedly different, are presented in this paper. The test procedure followed is exactly the same as explained in the previous section.

Tables 3 and 4 show the densities and rheology of the muds and their corresponding spacer fluids. **Figs. 10 and 11** illustrate the results for Mud 1 (16 lb/gal) and Mud 2 (10 lb/gal), respectively. The contact time necessary for cleaning the OBM film from the electrode is 4 min for Mud 1 and almost 19 min for cleaning Mud 2. These two muds are of the same base-oil and oil-water ratio, but different densities.

This is an example which clearly indicates that different OBMs require different amounts of spacer volumes for their cleaning and displacement. The present industry practice is to use general rules of 10 min of contact time or 1000 ft. of annular fill. Using this new technique, to quantify the contact

time necessary for the complete cleaning of the casing surface under given wellbore conditions, and the channel volumes obtained from a 3D displacement simulator, the spacer volumes to be used for a given cementing job can be custom-designed, thereby helping to ensure better quality of downhole assurance.

Table 3—Density and Rheology of Mud and Spacer for Set 1

	OBM	Spacer
Base oil	Mineral oil	—
Density, lb/gal	16	17
YP, lbf/100 ft^2	17	20
PV, cP	45	47

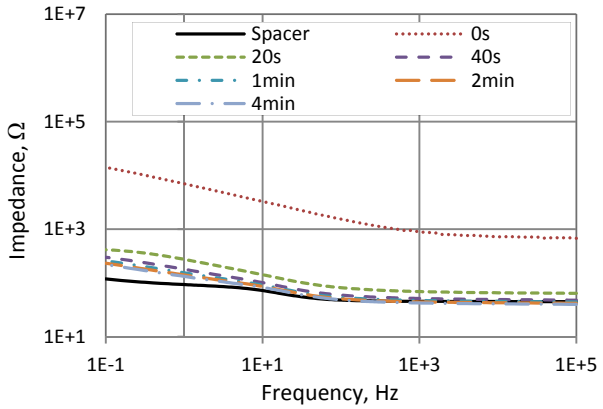

Fig. 10—EIS data log for 16 lb/gal mud.

Table 4—Density and Rheology of Mud and Spacer for Set 2

	OBM	Spacer
Base oil	Mineral oil	—
Density, lb/gal	10	12
YP, lbf/100 ft^2	17	20
PV, cP	25	28

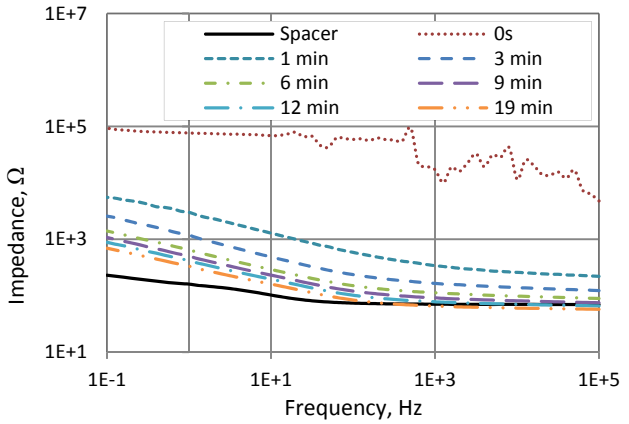

Fig. 11—EIS data log for 10 lb/gal mud.

The contact time for cleaning depends on various factors, such as the pump rate, surfactant concentration, type of OBM, and geometrical parameters of the wellbore. Using the previously described technique and a 3D displacement simulator,[21] the total spacer volume necessary for achieving complete mud-displacement and maintaining contact time for casing surface cleaning under various pump rates, can be obtained. Repeating this procedure by changing the parameters, such as pump rates, surfactant loading in the spacer fluids, etc., the cementing job can be properly engineered for a specific requirement.

Conclusions

To achieve a successful zonal isolation, preparing the wellbore for receiving the cement slurry is crucial. A new technique to quantify the wetting characteristics of the casing surface is described. The concept of double-layer capacitance and how it can be used to differentiate an oil-wet surface from a water-wet surface is detailed. The basics of EIS are explained with a description of how to model the data to analyze the physical system.

A set of results are explained to prove the concept. A detailed procedure for estimating the contact time to be maintained between the spacer fluid and casing for the thorough cleaning of the surface is explained. The results presented in this paper suggest that each mud is different and demands a different amount of spacer to prepare the wellbore for receiving the cement. Because the technique explained is non-invasive, the same experiment can be performed at the desired HP/HT conditions with carefully designed equipment adhering to safety standards.

Acknowledgments

The authors thank Chris Gordon for his valuable support and encouragement in performing these studies. The authors also thank Krishna Babu Yerubandi for his valuable inputs and discussions, as well as Sameer Bardapurkar for his help in building the experimental prototype. The authors also thank the management of Halliburton for the support in performing this study and for permission to publish this work.

Nomenclature

EIS = *Electrochemical impedance spectroscopy*
HP/HT = *High-pressure/high-temperature*
NAF = *Non-aqueous film*
OBM = *Oil-based mud*
RSS = *Residual shear stress*
SBS = *Shear bond strength*
WBM = *Water-based mud*

References

1. Rossen, W.R. and Kohn, J.P. 1984. Behavior of Microemulsions Under Compression. *Society of Petroleum Engineers Journal.* ***24*** (5): 536–544. SPE-11210-PA.
2. Quintero, L., Jones, T., Clark, D.E., Torres, C., and Christian, C. 2007. Single-phase Microemulsion Technology for Cleaning Oil or Synthetic-Based Mud. Paper AADE-07-NTCE-18 presented at the AADE National Technical Conference and Exhibition, Houston, Texas, USA, 10–12 April.
3. Robbins, M.L. 1976. Theory of the Phase Behavior of Microemulsions. Paper SPE 5839 presented at the SPE Improved Oil Recovery Symposium, Tulsa, Oklahoma, USA, 22–24 March.
4. Patel, A.D., Wilson, J.M., and Loughridge, B.W. Impact of Synthetic-Based Drilling Fluids on Oilwell Cementing Operations. Paper SPE 50726 presented at the SPE International Symposium on Oilfield Chemistry, Houston, Texas, USA, 16–19 February.
5. Lyons, W.C. 1996. Standard Handbook of Petroleum and Natural Gas Engineers. Houston, Texas: Gulf Publishing Company.
6. Heathman, J., Wilson, J.M., Cantrell, J.H, and Gardner, C. 2000. Removing Subjective Judgment from Wettability Analysis Aids Displacement. Paper SPE 59135 presented at the IADC/SPE Drilling Conference, New Orleans, Louisiana, USA, 23–25 February.
7. Osode, P.I., Otaibi, M.A., El-Kilany, K.A., Binmoqbil, K.H., and Azizi, E.S. 2012. Evaluation of Non-Reactive Aqueous Spacer Fluids for Oil Based Mud Displacement in Open Hole Horizontal Wells. Paper SPE 161914 presented at the Abu Dhabi International Petroleum Conference and Exhibition, Abu Dhabi, UAE, 11–14 November.
8. Olowolagba, K.O. and Yerubandi, K.B. 2011. Improved Spacer Rheology Model for Cement Operations, Paper SPE 140805 presented at the SPE Production and Operations Symposium, Oklahoma, City, Oklahoma, USA, 27–29 March.
9. Maserati, G., Daturi, E., Gaudio, L.D., Belloni, A., Bolzoni, S., Lazzari, W., and Leo, G. 2010. Nano-emulsions as Cement Spacer Improve the Cleaning of Casing Bore During Cementing Operations. Paper SPE 133033 presented at the SPE Annual Technical Conference and Exhibition, Florence, Italy, 19–22 September.
10. Zamora, M., Foxenberg, W., and Roy, S. 2006. Predicting Mud-Removal Efficiency During Completion-Fluid Displacements. Paper AADE-06-DF-HO-21 presented at the AADE Drilling Fluids Technical Conference, Houston, Texas, USA, 11–12 April.
11. Evans, G. and Carter, G. 1964. New Technique for Improving Cement Bond. Paper API-64-033 presented at the Drilling and Production Practice, New York, New York, USA, 1 January.
12. Carter, L.G. and Evans, G.W. 1964. A Study of Cement-Pipe Bonding. *Journal of Petroleum Technology*. **16** (2): 157–160. SPE-764-PA.
13. Scott, J.B. and Brace, R.L. 1966. Coated Casing–"A Technique for Improved Cement Bonding." Paper API-66-043 presented at the Drilling and Production Practice, New York, New York, USA, 1 January.
14. Israelachvili, J. 2011. Intermolecular and Surface Forces, third edition. Academic Press.
15. Basics of Electrochemical Impedance Spectroscopy http://www.gamry.com/application-notes/basics-of-electrochemical-impedance-spectroscopy/ accessed on 12th Feb 2014.
16. Loveday, D., Peterson, P., and Rodgers, B. 2004. "Evaluation of organic coatings with electrochemical impedance spectroscopy, Part 1: Fundamentals of Electrochemical Impedance Spectroscopy" *JCT Coatings Tech*, 8: 46-52
17. Loveday, D., Peterson, P., and Rodgers, B. 2004. "Evaluation of organic coatings with electrochemical impedance spectroscopy, Part 2: Application of EIS to Coatings" *JCT Coatings Tech*, 1(10), 88-93
18. Loveday, D., Peterson, P., and Rodgers, B. 2005. "Evaluation of organic coatings with electrochemical impedance spectroscopy, Part 3: Protocol of Testing Coatings with EIS" *JCT Coatings Tech*, 2(13): 22-27
19. Lasia, Andrzej. 1999. Electrochemical Impedance Spectroscopy and its Applications. Academic/Plenum Publishers. **32**: 143–248.
20. Taylor-Couette Flow, Richard Lueptow, http://www.scholarpedia.org/article/Taylor-Couette_flow accessed on 12th Feb 2014.
21. Savery, M., Chin, W., and Yerubandi, K.B. 2008. Modeling Cement Placement Using a New 3-D Flow Simulator. Paper AADE-08-DF-HO-08 presented at the AADE Fluids Conference and Exhibition, Houston, Texas, USA, 8–9 April.